CHAPTER 6

FURTHER PREDICTIONS ABOUT WELD METAL STRENGTH

6.1 INTRODUCTION

In general, when the volume fractions of the different phases are similar, a "rule of mixtures" is believed to be quite a good way of calculating strength (Ion *et al.*, 1984; Ashby, 1987). Thus, it should be possible to model the yield strength of a weld as the sum of the products of the volume fractions of the three principal phases and their stresses at yielding. In fact, work showed that direct analysis of this sort on its own is inadequate, and does *not* give satisfactory results. This is because the composition of the alloy must also be taken into account.

In Chapter 5, it was shown that the strength of a weld can be factorised into components due to the intrinsic strength of iron, solid solution strengthening, and the contributions from the three major phases (α, α_w, α_a) which constitute the microstructure, *i.e.*

$$\sigma_y = \sigma_{\mathrm{Fe}} + \sum_{i=1}^{k} \sigma_{\mathrm{SS}_i} + \sigma_\alpha v_\alpha + \sigma_a v_a + \sigma_w v_w \tag{6.1}$$

where σ_{Fe} is the strength of fully annealed pure iron as a function of temperature and strain rate,

σ_{SS_i} is the solid solution strengthening due to an alloying element i,

and σ_α, σ_a, and σ_w are the microstructural strength contributions, and v_α, v_a, and v_w are the volume fractions of the allotriomorphic, acicular, and Widmanstätten ferrite phases respectively.

This work is concerned with the further validation and development of this model, and involves the examination of a much larger number of welds. The ability to predict strength as a function of temperature is also investigated in this chapter.

6.2 EXPERIMENTAL METHOD

To test this model, three low-carbon manganese multipass welds were fabricated from 20mm thick plate using the manual-metal-arc welding process according to ISO–2560–1973 specifications. An ISO-2560 specification was used, since it is a joint geometry that leaves much of the weld metal free from dilution by the parent plate. The welding voltage was 23V (DC +ve) and a current of 180A was used. The net heat input was approximately 1.5 kJ/mm, and the maximum interpass temperature was 250°C. The welding speed was approximately 4 mm/s. The number of beads per weld was typically 25, each layer consisting of some three beads. The carbon content was manipulated using specially developed experimental electrodes, so that significantly different weld metal microstructures would evolve, the effect of increasing the carbon content being to increase the amount of acicular ferrite at the expense of allotriomorphic and Widmanstätten ferrite (Evans, 1981). Weld metal chemical analyses are given in Table I.

Weld	Composition, wt%											ppm by wt.	
ID.	C	Mn	Si	P	S	Cr	Ni	Mo	V	Ti	Al	N	O
6.1	0.043	1.25	0.43	0.017	0.008	0.02	0.02	0.005	0.002	0.010	0.002	72	394
6.2	0.10	1.56	0.42	0.015	0.007	0.04	0.04	0.01	0.006	0.013	0.015	119	262
6.3	0.15	1.57	0.45	0.012	0.007	0.04	0.03	0.01	0.008	0.014	0.015	96	193

Table 6.1: Weld metal analyses.

Figure 6.1 illustrates the welding procedure used, and shows the macrostructure of Weld 6.1.

Figures 6.2a and b contrast the as–welded and reheated regions. A trace of the original columnar morphology can still be seen. It can be seen that reheating changes the microstructure considerably. Subsequent passes, however, (Fig. 6.2c) have little obvious effect, although some slight increase in grain size was discernable. The amount of reheated weld metal was estimated by superimposing a grid of 6500 squares on it and then using areal analysis, and was found to be 54% (27% acicular ferrite), although the error associated with this estimate may be greater than is statistically implied because of the difficulty in distinguishing the as–welded and reheated regions (Gretoft and Svensson, 1986).

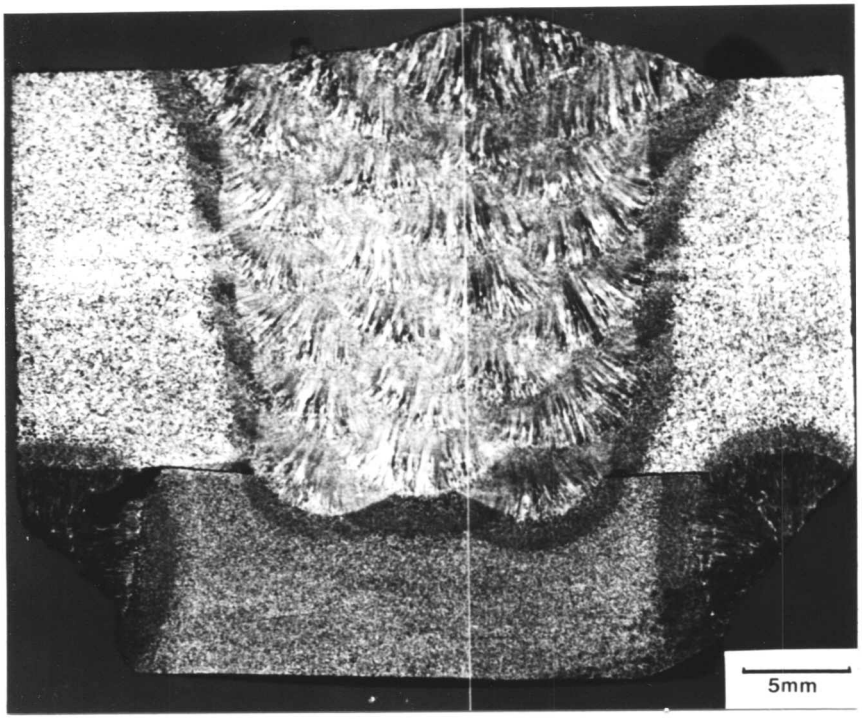

Figure 6.1: Weld 6.1: Cross-section of the weld deposit. Etchant: Ground and swab etched (unpolished) in ammonium thiosulphate.

a)

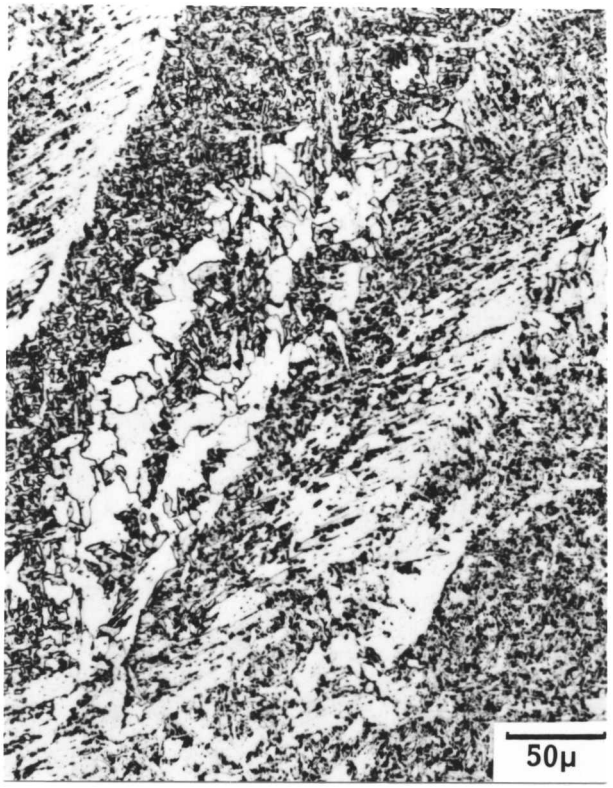

b)

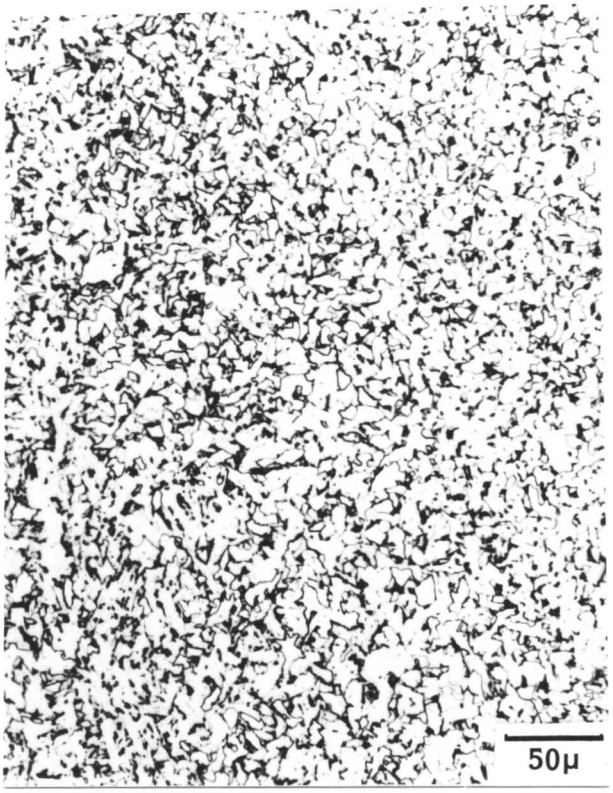

c)

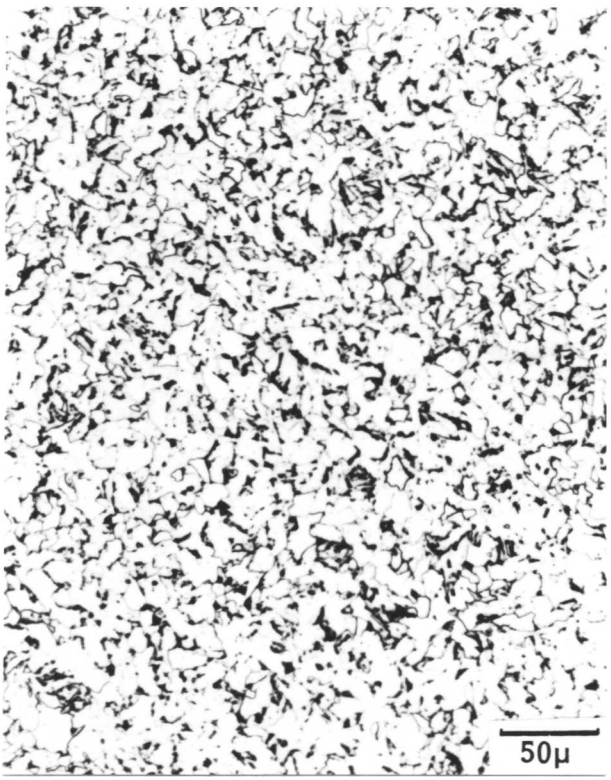

Figure 6.2: (a) As–welded and, (b) reheated and (c) double normalised (*i.e.* twice reaustenitised) weld regions. Etchant: 2% Nital.

Vickers hardness measurements (10 kg) were carried out in both the columnar (top bead) and reheated regions of the welds. Ten indentations were made for each measurement. The volume fractions of the phases present in the primary microstructure (top bead) were determined at 250× magnification using a Swift point counter. 1000 points were taken for each specimen. Quantitative metallographic data are given in Table 6.2.

Weld	Hardness (HV10)		Volume Fractions		
ID.	Primary	Reheated	v_α	v_w	v_a
1	200	171	0.30	0.11	0.59
2	232	212	0.22	0.11	0.67
3	252	241	0.18	0.06	0.76

Table 6.2: Metallographic and hardness results for primary microstructure.

6.3 THE DETERMINATION OF YIELD STRESS FROM HARDNESS

A considerable amount of published work deals with the strength of multirun welds as a whole, whereas this work is concerned initially with just the primary microstructure for which property data other than hardnesses are not common. However, it is possible to estimate the yield strength of the primary weld microstructure from the hardness. For a rigid-plastic material indented by a Vickers indenter, the 0.2% offset yield strength is given by (Cahoon *et al.*, 1971)

$$\sigma_y = \left(\frac{H}{3}\right)(0.1)^{(m-2)} \tag{6.2}$$

where H is the hardness

and m is the Meyer's hardness coefficient.

It has been shown theoretically, and confirmed experimentally (Tabor, 1951), that

$$n = m - 2 \tag{6.3}$$

where n is the strain-hardening exponent for the material.

Therefore, combining Eqns. 6.2 and 6.3 gives

$$\sigma_y = \left(\frac{H}{3}\right)(0.1)^n \tag{6.4}$$

n is indicative of the material's ability to work-harden (*e.g.* for pure iron, $n = 0.31$ (Davies, 1978); for a low carbon annealed steel, $n = 0.26$ (Low and Garofalo, 1947)). For a severely cold-worked material n may be taken as zero, when (Bowden and Tabor, 1964)

$$\sigma_y \simeq \frac{H}{3} \tag{6.5}$$

This simple relationship was applied to see if it would allow weld metal yield strength to be predicted from hardness measurements, but was found to consistently overestimate the weld metal yield strength. This is because the as-welded microstructure still retains some work-hardenability, and thus Eqn. 6.4 should be used. In fact, empirical relationships between the hardness and yield strength already exist (Hart, 1975; Pargeter, 1978). However, as Pargeter (1978) noted, simple correlations between hardness and yield strength will necessarily be inaccurate, because of the complexity of weld metal behaviour in a hardness test. Also, the strain-hardening coefficient, n, will not be a fixed value, but will be influenced by the hardness of the weld metal itself. However, an estimate for n as a function of microstructure could be made using the values obtained for K and n for the individual microstructural constituents in Chapter 5.

Let

$$\sigma = K\epsilon^n \tag{6.6}$$

Then

$$\frac{\sigma_y}{\sigma_{UTS}} = \frac{{\epsilon_y}^n}{{\epsilon_{UTS}}^n} \tag{6.7}$$

which, employing the assumptions made earlier ($\epsilon_y = 0.002$; $\epsilon_{UTS} \equiv n$) becomes

$$\frac{\sigma_y}{\sigma_{UTS}} = n^{-n}(0.002)^n \tag{6.8}$$

σ_y and σ_{UTS} were determined from Eqn. 5.22.

n was then found by solving Eqn. 6.8 iteratively using the Newton-Raphson technique (Kreyzig, 1972). An estimate of the strength of the weld from its hardness could then be made by substituting the value obtained into Eqn. 6.4.

The variation due to the change in the strength of pure iron, and the solid solution strengthening were then subtracted for each weld to give the strengthening due to microstructure. These calculations are summarised in Table 6.3. The hardnesses are high since it is the primary columnar region that is being considered.

Weld ID.	VHN	σ_y MPa	$\sigma_{\text{Fe}} + \sum_{i=1}^{k} \sigma_{\text{SS}_i}$ MPa	σ_{micro} MPa
6.1	200	573	362	211
6.2	232	668	389	279
6.3	252	725	383	342

Table 6.3: Strength analysis of the primary weld microstructure.

From the results of Chapter 5, the strengthening due to allotriomorphic ferrite is expected to be appreciably less than that of the Widmanstätten and acicular ferrite phases, which should have approximately similar strengths. Both have morphologies giving them a smaller effective grain size than allotriomorphic ferrite. This is further suggested by the increase in hardness in Welds 6.1–3, which can be connected directly with the increase in the amounts of acicular ferrite in the welds (see Table 6.2). Thus, it is expected that σ_α will be less than both σ_a and σ_w.

As an additional experiment, Welds 6.1, 6.2, and 6.3 were heat-treated at 700°C for 50 hours. This prolonged heat treatment would have the effect of annealing the microstructure, and so σ_{micro} should be nearly zero. The heat-treated welds are designated with the suffix R. After the heat treatment, the hardnesses of the

specimens were as follows:

Weld 6.1R: 125 HV
Weld 6.2R: 136 HV
Weld 6.3R: 133 HV

The interpretation of these results is given below.

6.4 METHOD OF ANALYSIS

In order to calculate σ_α, σ_a, and σ_w, the results from Table 6.3 were collated with data from 78 other welds from a variety of sources (Abson, 1978; Abson, 1982; Cunha *et al.*, 1982; Bailey, 1985; McRobie and Knott, 1985; Lathabai and Stout, 1987; Thewlis, 1987), combining data for 15 submerged-arc and 19 manual-metal-arc welds (Abson, 1978; Abson, 1982; Cunha *et al.*, 1982; McRobie and Knott, 1987), 7 flux-cored arc welds (Lathabai and Stout, 1987), and 37 triple arc submerged-arc welds (Bailey, 1985; Thewlis, 1987). For all the welds cited, their composition, the volume fractions of the microstructural constituents in the primary regions, and their hardness data are all available. The precise welding conditions used vary considerably –for example, the arc energies associated with the different techniques vary by more than an order of magnitude from 0.7kJ/mm Abson (1982) to 20kJ/mm (Bailey, 1985), and preheat temperatures vary from room temperature to 250°C– but these differences are reflected in the different microstructures that evolve. Idiomorphic ferrite, comprising typically <1%, in Abson (1982), was counted as allotriomorphic ferrite for the present work. It should be mentioned that in Cunha *et al.* (1982), Welds 3 and 4 were ignored since the stated volume fractions of the phases present did not add up to unity. Also, their definition of proeutectoid ferrite in the welds whose volume fractions were given, showed they, in fact, meant allotriomorphic ferrite, and it was treated as such.

Since v_α, v_a, and v_w are not independent v_w was written as $(1-v_\alpha-v_a)$ during the factorisation of the microstructure component of strength. σ_{micro} could then be solved as:

$$\sigma_{\text{micro}} = x + y(v_\alpha) + z(v_a) \tag{6.9}$$

Table 6.1 contd.

Lathabai and Stout, 1987	F2	240	701	362	0.09	0.02	0.89
"	F1	226	660	346	0.10	0.08	0.82
"	F5	215	628	347	0.14	0.02	0.84
"	M2	247	721	362	0.11	0.01	0.88
"	M1	228	666	333	0.20	0.05	0.75
"	M6	205	598	351	0.21	0.01	0.78
"	M5	179	523	323	0.39	0.13	0.48
Thewlis, 1987	22A11	191	558	307	0.25	0.04	0.71
"	22A12	195	569	308	0.23	0.02	0.75
"	22A13	191	558	308	0.24	0.01	0.75
"	22A14	198	578	326	0.21	0.00	0.79
"	22A15	197	575	315	0.19	0.00	0.81
"	22A16	195	569	314	0.21	0.00	0.79
"	22A17	208	607	317	0.21	0.06	0.73
"	22A18	208	607	316	0.21	0.03	0.76
"	22CA1	198	578	326	0.21	0.00	0.79
"	22CA2	203	593	311	0.24	0.00	0.76
"	22NCA1	195	569	311	0.20	0.01	0.79
"	22NCA2	195	569	312	0.24	0.01	0.75
"	22N1	198	578	326	0.21	0.05	0.74
"	22N2	199	581	342	0.22	0.00	0.78
"	22N3	206	601	341	0.23	0.00	0.77
"	22N4	204	596	347	0.25	0.00	0.75
"	33A11	193	563	312	0.14	0.00	0.86
"	33A12	192	561	316	0.15	0.01	0.84
"	33A13	205	598	315	0.16	0.00	0.84
"	33A14	206	601	334	0.14	0.01	0.85
"	33A15	200	584	320	0.13	0.00	0.87
"	33A16	198	578	312	0.15	0.01	0.84
"	33A17	208	607	316	0.09	0.02	0.89
"	33A18	205	598	317	0.03	0.36	0.61
"	33CA1	206	601	334	0.14	0.00	0.86
"	33CA2	200	584	320	0.15	0.00	0.85
"	33NCA1	202	590	319	0.17	0.01	0.82
"	33NCA2	205	598	320	0.18	0.00	0.82
"	33N1	196	572	323	0.10	0.01	0.89
"	33N2	206	601	334	0.14	0.00	0.86
"	33N3	199	581	335	0.15	0.00	0.85
"	33N4	200	584	338	0.17	0.00	0.83
"	33N5	212	619	340	0.18	0.00	0.82
"	33N6	205	598	339	0.21	0.05	0.74
This work	6.1	200	584	362	0.30	0.11	0.59
"	6.2	232	677	389	0.22	0.11	0.67
"	6.3	252	736	383	0.18	0.06	0.76

Table 6.4: Summarising the data used in the calculation of yield strength and solid solution strengthening as a function of microstructure.

Reference	Weld ID.	VHN	σ_y MPa	$\sigma_{Fe} + \sum_{i=1}^{k} \sigma_{SS_i}$ MPa	V_α	V_w	V_a
Abson *et al.*, 1978	OP1211	218	636	334	0.10	0.05	0.85
"	OP1212	207	604	334	0.18	0.03	0.79
"	OP1213	188	549	326	0.15	0.06	0.79
"	OP1214	188	549	324	0.16	0.05	0.79
"	801	214	625	357	0.12	0.59	0.29
"	802	202	590	343	0.24	0.62	0.14
"	803	188	549	335	0.11	0.74	0.15
"	804	184	537	329	0.18	0.63	0.19
Abson, 1982	W8SS	217	640	387	0.20	0.27	0.53
"	W8R	236	695	382	0.16	0.21	0.63
"	W9SS	244	719	405	0.09	0.14	0.77
"	W9R	259	763	416	0.10	0.11	0.79
"	W7SS	251	740	415	0.05	0.06	0.89
"	W7R	256	754	414	0.10	0.11	0.79
"	W14SS	237	698	401	0.12	0.08	0.80
"	W14R	220	648	419	0.23	0.14	0.63
Cunha *et al.*, 1982	1	204	599	347	0.28	0.17	0.55
"	2	225	660	374	0.42	0.33	0.25
"	5	219	643	384	0.18	0.09	0.73
"	6	200	587	346	0.30	0.25	0.45
"	7	196	575	353	0.29	0.12	0.59
"	8	190	557	384	0.25	0.27	0.48
"	9	202	593	375	0.19	0.02	0.79
"	10	187	549	367	0.32	0.13	0.55
"	11	226	663	393	0.24	0.03	0.73
"	12	198	581	387	0.24	0.18	0.58
"	13	184	539	361	0.35	0.24	0.41
"	14	266	780	373	0.08	0.92	0.0
"	15	227	666	389	0.18	0.03	0.79
"	16	212	622	351	0.25	0.18	0.57
"	17	204	599	359	0.24	0.07	0.69
"	18	202	593	347	0.22	0.07	0.71
"	19	187	548	335	0.36	0.44	0.20
Bailey, 1985	W1	212	621	362	0.20	0.26	0.54
"	W2	210	615	357	0.18	0.13	0.69
"	W4	222	650	357	0.13	0.02	0.85
McRobie and Knott, 1985	A	187	546	353	0.42	0.04	0.54

Contd. overleaf.

where $x = \sigma_w$

$$y = (\sigma_\alpha - \sigma_w)$$

and $z = (\sigma_a - \sigma_w)$

x, y, and z were then found by linear regression of σ_{micro} against v_α and v_a for the 81 welds (Draper and Smith, 1966). The regression analysis works to minimize the deviance of the data, where the deviance

$$\mathrm{D} = \sum_{i=1}^{k} \{\sigma_{\text{micro}} - x - y(V_\alpha) - z(V_a)\}^2 \tag{6.10}$$

The overall method for determining σ_α, σ_a, and σ_w is summarised in Figure 6.3. The hardness is used to calculate the yield strength, from which is subtracted the strength of pure iron, and solid solution strengthening to give σ_{micro}. Combining this with the volume fractions of the phases present allows σ_α, σ_{a}, and σ_w to be calculated. Regression analysis was performed using the Royal Statistical Society's GLIM† (Generalised Linear Interactive Modelling) software.

6.5 RESULTS

Eqn. 6.9 was solved to give (with standard errors):

$$x = 325 \pm 30 \text{ MPa}$$
$$y = -317 \pm 68 \text{ MPa}$$
$$\text{and } z = -0.19 \pm 29 \text{ MPa}$$

Eqn. 6.1 may therefore be written as:

† ©NAG Central Office, 7 Banbury Road, Oxford, U.K.

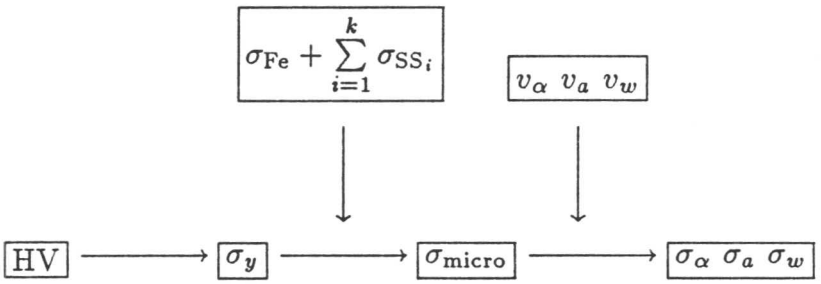

Figure 6.3: Flow diagram illustrating the steps involved in factorising the strength.

$$\sigma_y = \sigma_{\mathrm{Fe}} + \sum_{i=1}^{k} \sigma_{\mathrm{SS}_i} + 8V_\alpha + 325V_w + 325V_a \text{ MPa} \qquad (6.11)$$

Figure 6.4 shows a comparison between the observed yield strengths of the primary microstructure against those predicted using Eqn. 6.11.

After 50 hours at 700°C, the microstructures of Welds 6.1R, 6.2R, and 6.3R all showed plain columnar grains containing inclusions. As an example, Figure 6.3 shows the microstructure of Weld 6.1 before and after heat treatment. In Figure 6.3b, the grains still retain their columnar morphology, but the as-deposited weld microstructure has recrystallized to leave a uniform microstructure within the grains. Thus, although there may be a small strengthening effect due to grain size, σ_{micro} should be rather small.

As with the other results, the strain-hardening exponents for the heat-treated specimens were calculated using Eqn. 6.8. (To calculate σ_{UTS}, it was assumed that the heat-treated microstructures comprised 100% α. This assumption is fair, since at the yield stress, σ_α is almost negligible, and allows an estimate of the ultimate tensile strengths of the annealed welds). σ_y has been taken as $\sigma_{\mathrm{Fe}} + \sum_{i=1}^{k} \sigma_{\mathrm{SS}_i}$. The results of the calculation of the hardnesses of the welds are given in Table 6.4.

Weld ID.	σ_y/MPa	VHN (Measured)	VHN (Calculated)
6.1	362	125	129
6.2	389	136	137
6.3	383	133	135

Table 6.5: Measured and calculated values of the hardness of welds 6.1R-3R, reheated at 700°C for 50 hours.

6.6 DISCUSSION

The values obtained for σ_α, σ_w, and σ_a at yield compare extremely favourably, and are internally consistent, with those obtained in Chapter 5 (c.f. Eqn. 5.21a). In this Chapter, a much greater number of welds have been analysed, and the results

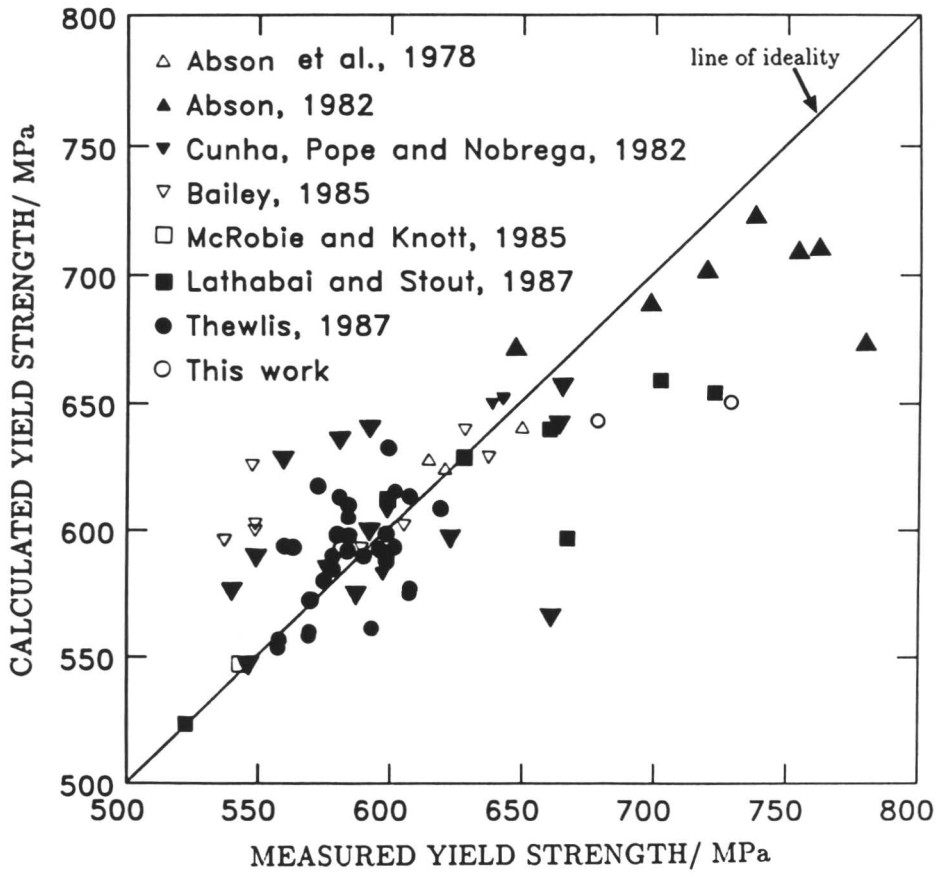

Figure 6.4: Comparison of observed yield strength of primary microstructure and that calculated by Eqn. 6.11. (Correlation coefficient = 0.81).

a)

b)

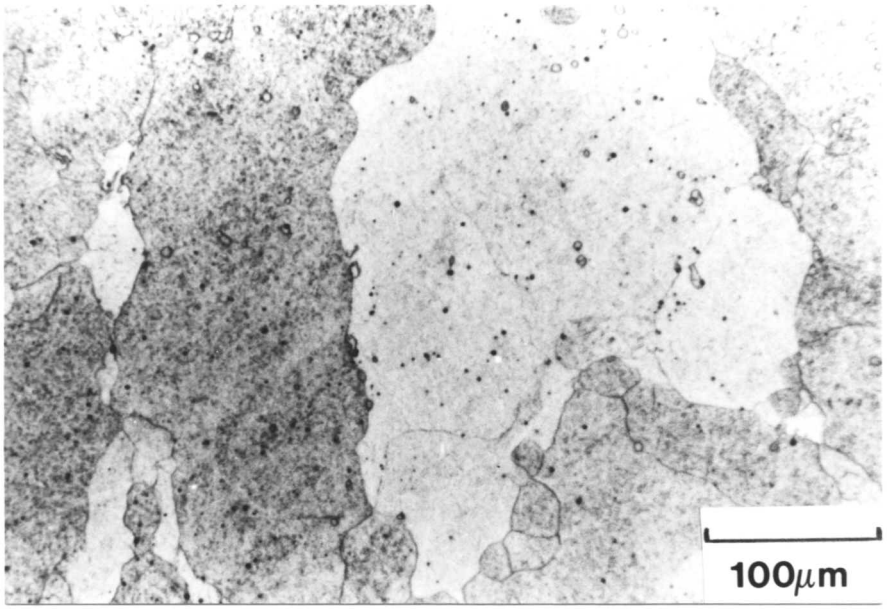

Figures 6.5a and b: (a) Weld 6.1: As-deposited weld metal adjacent to the fusion boundary, and (b) Weld 6.1R: After 50 hours at 700°C.

obtained, shown in Figure 6.4, demonstrate that this method works for a wide range of welds, irrespective of the welding process variables used. It can be seen that in Figure 6.4 the measured strengths are higher than the predicted strengths for higher strength welds. The most probable reason for this is that the effect of the microphases becomes more significant at higher strengths, and they then contribute noticeably to the microstructure. Since the microphases are primarily martensitic, they impart hardness to the weld and so raise the apparent strength. Indeed, it is this behaviour which perhaps ultimately limits the accuracy of this model. It should be noted that although σ_w and σ_a were found to be the same in this analysis (Eqn. 6.11), they will have different hardnesses, since their capacities to strain-harden are different. This is accounted for in Eqn. 6.4.

By adding back σ_{Fe}, it is also possible to calculate the hardness of the individual phases in a hypothetical unalloyed weld using Eqn. 6.3. For α, α_w, and α_a, the hardnesses are 86, 189 and 195 HV respectively, and are the minimum hardnesses that would be found in welds of homogeneous allotriomorphic, Widmanstätten or acicular ferrite. These values are considerably less than values found elsewhere (Chaveriat *et al.*, 1987), because the solid solution strengthening contribution has been removed.

The effect of annealing the welds for 50 hours at 700°C was to reduce σ_{micro} to a minimal value in each case. By taking the yield strength of the welds as being equal simply to the sum of the strength of pure annealed iron plus the solid solution strengthening due to alloying elements in the welds, it can be seen from Table 6.4 that it has been possible to predict the hardness of the annealed welds with extreme accuracy. This is a significant result, since, from the outset, one of the key aims of this work was to construct a model that would be able to describe weld metal strength as a function of thermal history, as well as composition, which is what has been done. It is interesting to note that, after annealing, Weld 6.2 possesses the highest strength, since microstructural strengthening is absent and it has the highest solid solution strengthening.

Now that a model has been constructed which allows weld metal strength to be calculated as a function of microstructure and heat treatment, this offers the possibility of being able to predict strength as a function of temperature, since it is now possible to calculate how the yield strength of pure iron, and the solid solution strengthening due to dilute alloying element additions varies with tem-

perature. This should be an exciting development, and is ultimately necessary to resolve many of the inconsistencies current in weld metal testing procedures. For example, although quality toughness tests are habitually carried out at a range of temperatures down to $-60°C$, tensile tests are nearly always carried out at room temperature, even though the strength of a weld is temperature dependent. As an illustration of this, Figure 6.6a shows how the strength of the annealed weld, Weld 6.1R, will vary with temperature over the range 100-750K. This is done using the experimental data and methods cited in Chapter 5. The resultant change in strength is complex because it is the summation of the individual effects of iron, with the alloying element additions that is being displayed. Nevertheless, it can be seen that with decreasing temperature, the yield strength of the weld increases considerably. This can be attributed principally to an increase in the yield strength of iron itself. Figures 6.6b, c, and d show variously how dilute additions of manganese, silicon, and nickel will then alter the strength of the weld. At room temperature and above, all three elements provide strengthening. However, at subzero temperatures, manganese, and especially nickel, are able to provide softening by disrupting the b.c.c. lattice so that dislocations lying in potential energy minima can glide more easily, making slip easier, although the exact mechanism by which this happens is not understood (Leslie, 1981). This behaviour makes them desirable alloying elements for low temperature applications. Nickel is also favourable at low temperatures from the point of view of toughness, since it increases the cleavage strength of ferrite (Jolley, 1968). A continuous representation of the effect of nickel on the yield strength of Weld 6.1R in the range 100-600K is given in Figure 6.7. Note the marked softening that occurs at reduced temperatures when nickel is present. In contrast, Figure 6.6c shows that silicon exhibits no real softening effect except at low temperatures. This work, therefore, offers the possibility that alloys could be designed specifically for the environments for which they are intended.

In fact, it is not yet possible to calculate how the yield strengths of *as-deposited* welds vary with temperature, since the primary microstructure of a weld metal contains a dislocation substructure (Tremlett *et al.*, 1961; Mandziej and Sleeswyk, 1987). This contributes to raise the strength of a weld above that of a steel of equivalent composition, and will comprise a major part of the microstructural strengthening component, σ_{micro}. Experimental work due to Whapham and Edwards [cited as ref. 13 in Judson and McKeown (1981)] apparently found there to be no difference in the dislocations densities of acicular ferrite, allotriomorphic

a)

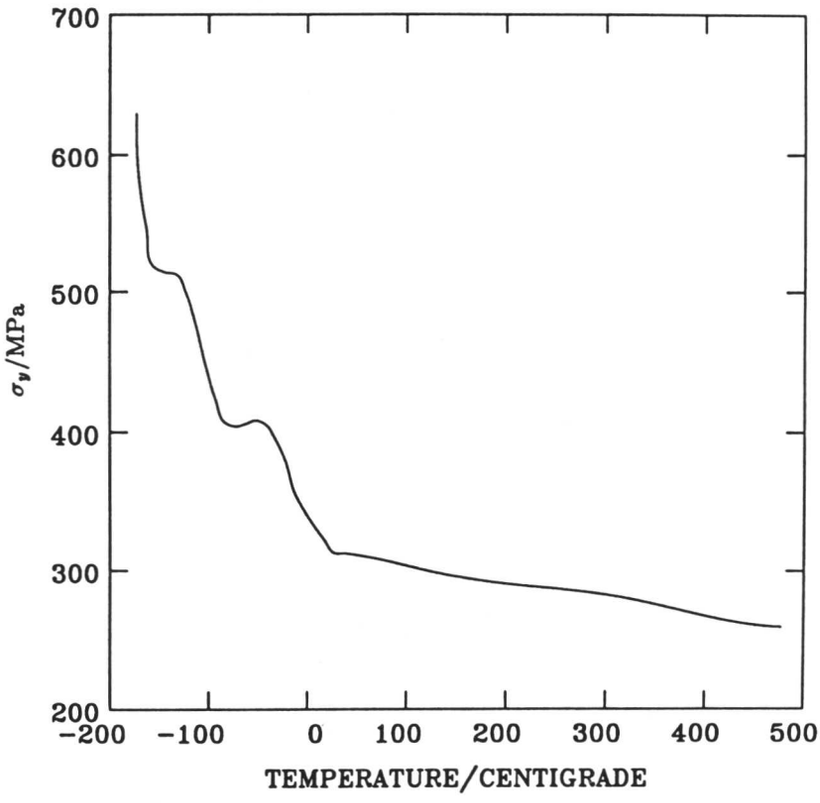
700
600
500
400
300
200
σ_y/MPa
−200
−100
0
100
200
300
400
500
TEMPERATURE/CENTIGRADE

b)

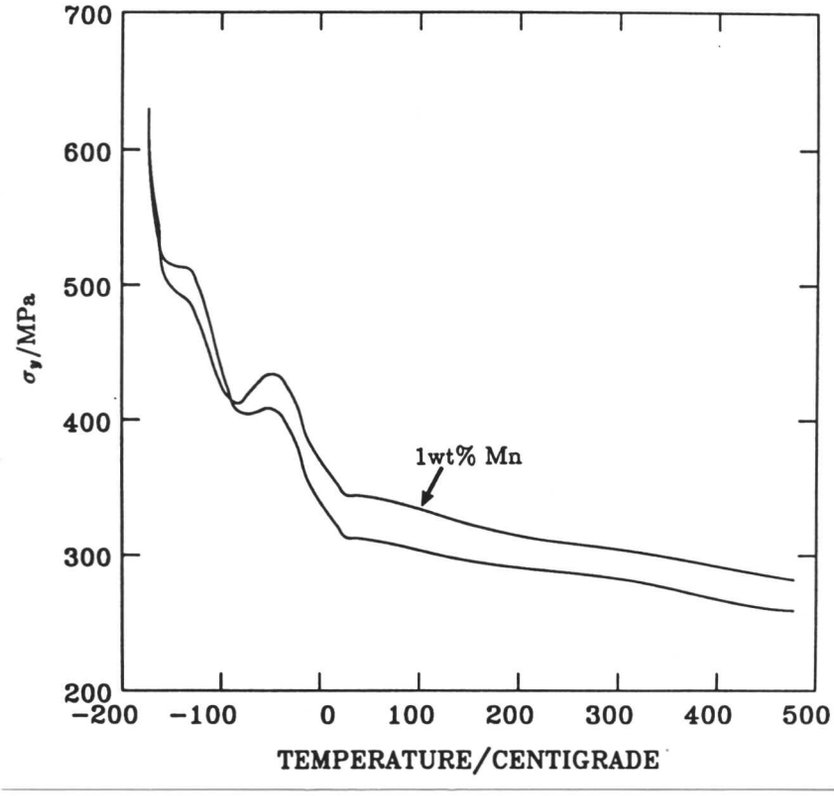
700
600
500
400
300
200
σ_y/MPa
1wt% Mn
−200
−100
0
100
200
300
400
500
TEMPERATURE/CENTIGRADE

c)

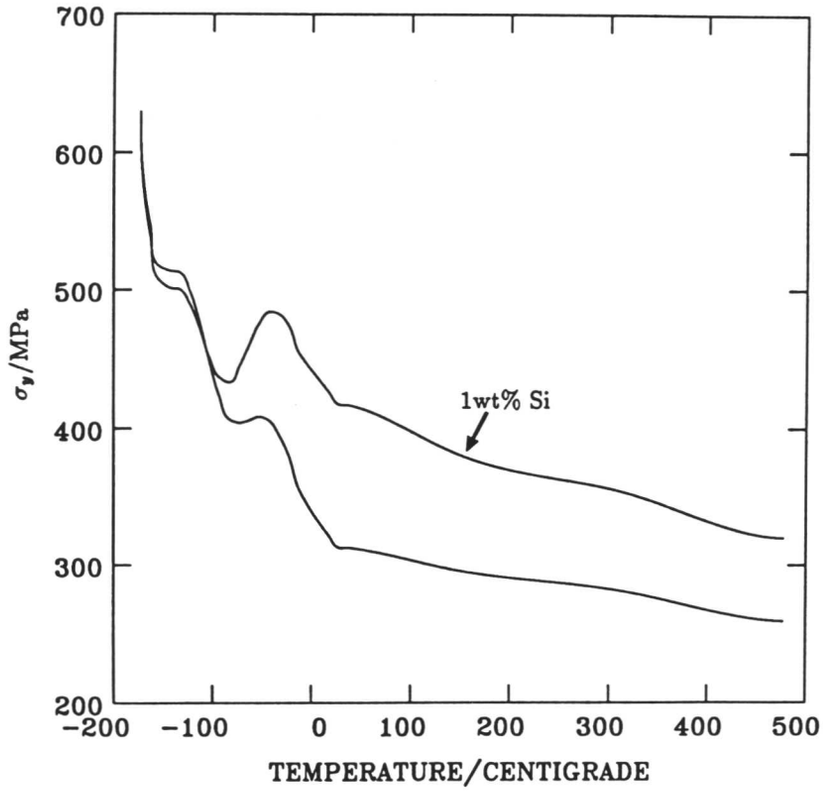

d)

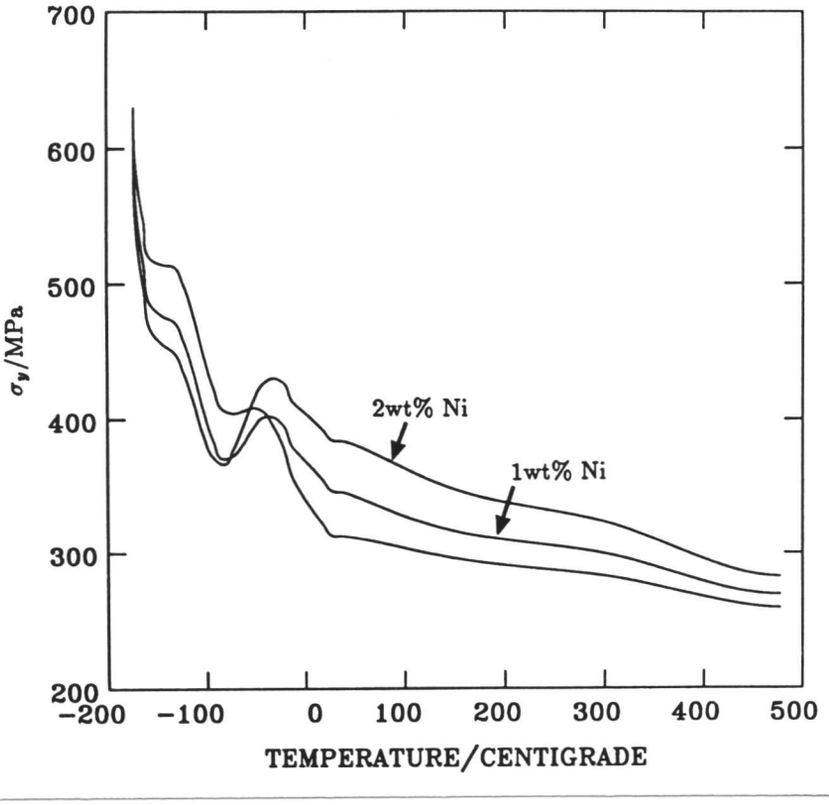

Figures 6.6a-d: Weld 6.1R: Calculation of the yield strength of annealed weld as a function of temperature. (a) As alloyed, and (b, c, and d) with manganese, silicon, and nickel additions respectively.

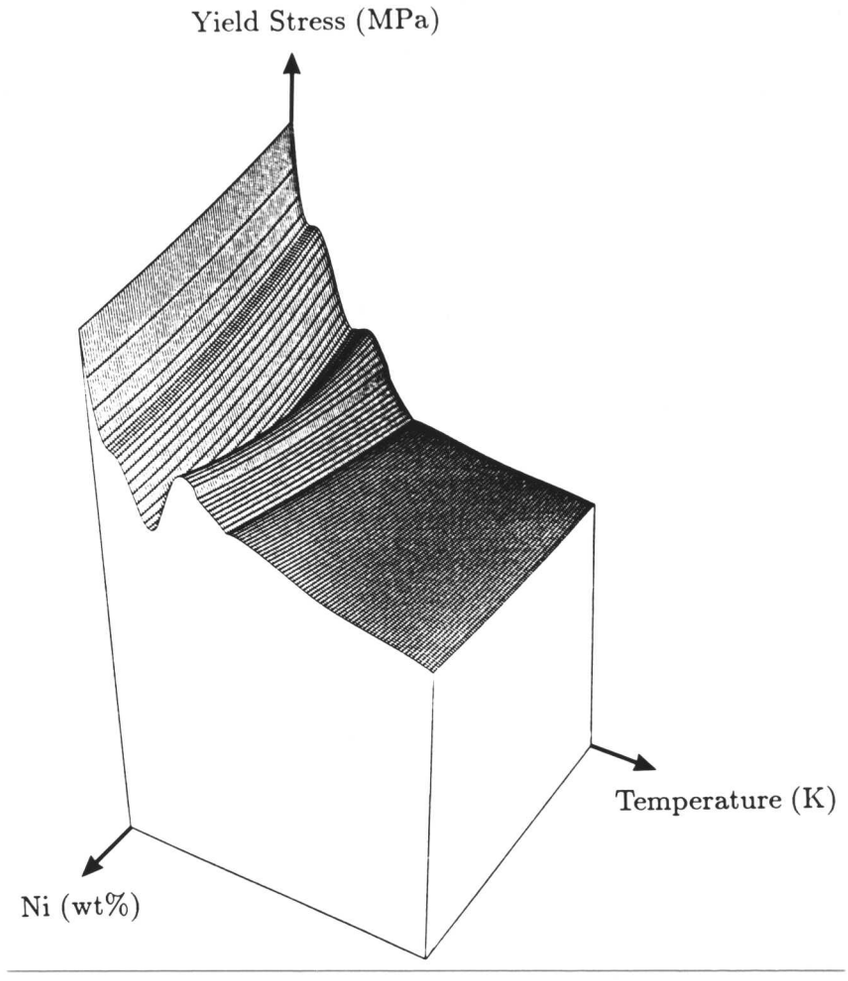

Figure 6.7: Weld 6.1R: The effect of increasing percentage nickel on the yield stress of an annealed weld as a function of temperature. (Ni: 0-2.5wt%; temperature: 100-600K; yield stress: 0-630MPa). The effect of adding nickel was calculated by interpolating experimental data due to Leslie (1972).

ferrite, and even the as-deposited and reheated regions of a weld examined in the TEM. The work cited is confidential, and so cannot be critically assessed. However, the results are extremely improbable. Microstructural strengthening is directly related to the dislocation density (Keh and Weissman, 1963), and the high values obtained for σ_w and σ_a in the preceding analysis, relative to σ_α, reflect in part the different dislocation densities found in the three phases. Widmanstätten ferrite and acicular ferrite grow by displacive transformation, and so will tend to have a higher dislocation density than allotriomorphic ferrite, which grows diffusionally (Bhadeshia *et al.*, 1985). In fact, acicular ferrite has indeed been found to have a relatively high dislocation density, of the order of $10^{14}\mathrm{m}^{-2}$ (Yang, 1987), conducive with this transformation mechanism. Since a decrease in the temperature of a steel will cause a decrease in dislocation mobility (Maekawa, 1972), it is evident that the microstructural contribution of the phases present to the overall strength of a weld metal will be temperature dependent. This will lead to a more pronounced increase in strength with decreasing temperature than with solid-solution-strengthened iron. Thus, the present work may be seen to provide a lower bound for predicting how the yield stress of a weld, of equal strength at room temperature, would alter with decreasing temperature.

As well as primary weld regions, multirun weld deposits contain areas of reheated microstructure. Since these regions should have a similar hardenability to the regions containing the primary microstructure, we would expect the hardness of the reheated regions to reflect that of the primary microstructure. Figure 6.8 shows results from Table 6.3 combined with data given in Abson (1982) and Cunha *et al.* (1982), and it can be seen that this is indeed the case. The offset along the x axis arises because the reheated regions will be consistently softer than the as-deposited regions. Recently, work, following on from this research, has been underway to predict the strength of multirun welds (Svensson *et al.*, 1988). This has been done by treating the microstructure as comprising reheated and as-deposited regions which contribute different amounts towards the overall weld metal strength. Although this method is approximate, it has, so far, produced reasonable quantitative results.

6.7 SUMMARY

Using published data for the hardnesses of the as-deposited regions of steel welds, together with data from three experimental welds, coefficients for the microstruc-

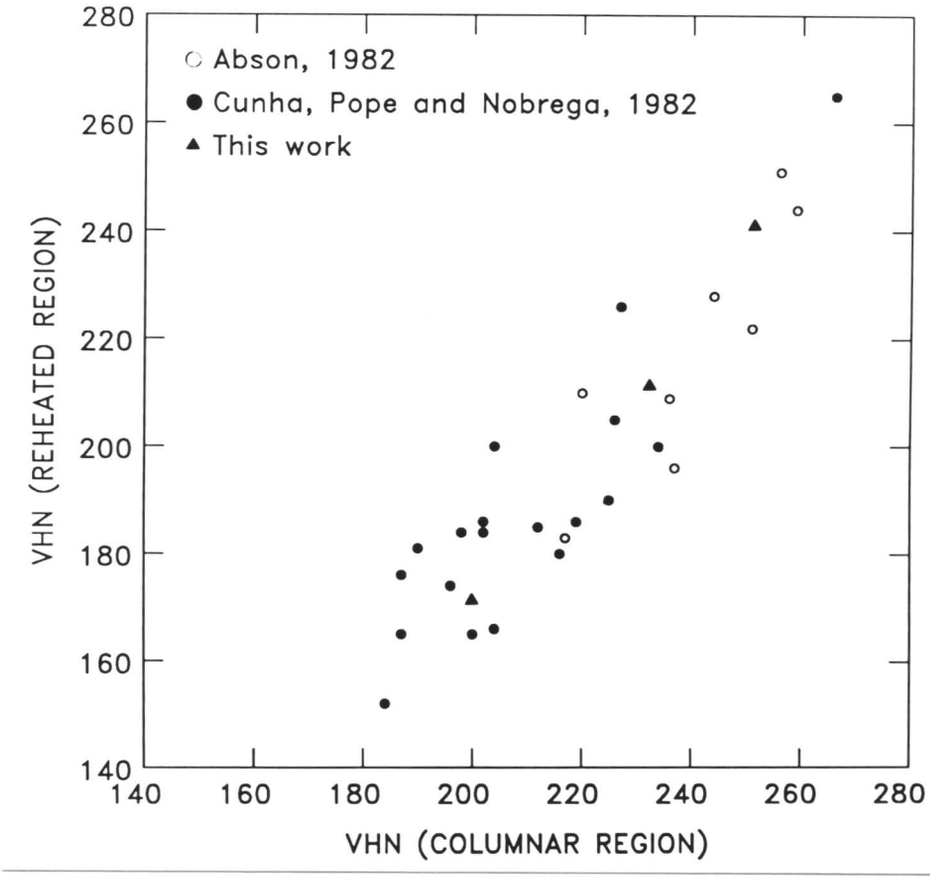

Figure 6.8: Comparing the hardnesses of the primary and reheated microstructures. (Correlation coefficient = 0.90.)

tural strengthening due to allotriomorphic ferrite, Widmanstätten ferrite, and acicular ferrite have been derived which are consistent with those obtained in Chapter 5, and confirm the model described above. This work also demonstrates that the yield strength of the primary microstructure of a weld can be estimated realistically from a knowledge of the volume fractions of the phases present, which are used to estimate the strain-hardenability of the weld metal, and its hardness.

Prolonged subcritical annealing of the three experimental welds, was found to remove the strengthening due to the as-deposited microstructure, the residual strength being found to be equal to the strength of pure annealed iron together with the solid solution strengthening due to the substitutional alloying elements present in the welds. Calculations of the effect of temperature on the strength of one of the welds revealed that at, and above, room temperature, manganese, silicon, and nickel additions all imparted strengthening. However, at low temperatures, softening was observed to occur with additions of nickel, and, to a lesser extent, with manganese and silicon additions, when these elements assist, rather than impede, slip. This work suggests, therefore, that additions of nickel are desirable to promote good mechanical strengthening in welds which are to be used at low temperatures. The possibilities of being able to predict quantitatively the as-welded yield strength of steel weld metals as a function of temperature, and the yield strength of multirun welds were also discussed.

REFERENCES

ABSON, D. J., (1982) *Weld. Inst. Res. Rep.*, Welding Institute, Abington, U. K., No. 194/1982.

ABSON, D. J., DOLBY, R. E., and HART, P. H. M. (1978), "Trends in Steels and Consumables for Welding", *[Proc. Conf.]* Welding Institute, Abington, U.K., paper 25.

ASHBY, M. F., (1987), Private Communication.

BAILEY, N, (1985) *Weld. Inst. Res. Rep.*, Welding Institute, Abington, U. K., No. 291/1985.

BHADESHIA, H. K. D. H., SVENSSON, L.–E., and GRETOFT, B., (1985) *Acta Metall.*, **33**, 1271–1283.

BOWDEN, F. P. and TABOR, D., (1964) "The Friction and Lubrication of Solids", Part II, 1^{st} Ed., Oxford Universitiy Press, London EC4, U. K., 324.

CAHOON, J. R., BROUGHTON, W. H., and KUTZAK, A. R., (1971), *Metall. Trans.*, **2**, 1971-1979.

CHAVERIAT, P. F., KIM, G. S., SHAH, S., and INDACOCHEA, J. E. (1987), "Metallography and Interpretation of Weld Microstructures", A. S. M. International, Metals Park, Ohio 44073, 195-226.

CUNHA, P. C. R., POPE, A. M., and NOBREGA, A. F., (1982) "Second International Conference on Offshore Welded Structures", *[Proc. Conf.]*, Welding Institute, Abington, U.K., paper 40.

DAVIES, R. G. (1978), *Metall. Trans. A*, **9A**, 451-455.

DRAPER, N. R. and SMITH, H., (1966) "Applied Regression Analysis", Wiley, New York.

EVANS, G. M., (1981) IIW Doc. II-A-546-81.

GRETOFT, B. and SVENSSON, L–E., (1986) IIW Doc. IX–1453–86.

HART, P. H. M. (1975), *Weld. Inst. Res. Bull.*, **16**, 176.

ION, J. C., EASTERLING, K. E., and ASHBY, M. F. (1984), *Acta Metall.*, **32**, (11), 1949-1962.

JOLLEY, W. (1968), *Trans. A. I. M. E.*, **242**, 306-314.

JUDSON, P. and McKEOWN, D. (1982), "2^{nd} International Conference on Off-

shore Welded Structures", *[Proc. Conf.]*, Welding Institute, Abington, U.K., paper 3.

KEH, A. S. and WEISSMAN, S. (1963), "Electron Microscopy, and the Strength of Crystals", Eds., G. Thomas and J. Washburn, Interscience, New York, 231.

KREYZIG, E. (1972), "Advanced Engineering Mathematics", 3rd Ed., Wiley, 638-639.

LATHABAI, S. and STOUT, R. D. (1987), "Microstructural Science", Eds., M. R. Louthan, Jr., I. LeMay, and G. F. Vander Voort, Elsevier Science Publishing Co., New York, **14**, 77-97.

LESLIE, W. C., (1972) *Metall. Trans.*, **3**, 5–26.

LESLIE, W. C. (1981), "The Physical Metallurgy of Steels", McGraw-Hill Book Co., New York, 115-119.

LOW, J. R. and GAROFALO, F. (1947), *Proc. Soc. Exp. Stress Anal.*, 4, (2), 16-25.

McROBIE, D. E. and KNOTT, J. F. (1985), *Mat. Sci. Tech.*, **1**, (5), 357-365.

MAEKAWA, I. (1972), "Mechanical Behaviour of Materials", *[Proc. Conf.]*, The Society of Materials Science, Japan, **3**, 127-134.

MANDZIEJ, S. and SLEESWYK, A. W. (1987), "Welding Metallurgy of Structural Steels," *[Proc. Conf.]*, The Metallurgical Society/AIME, 420 Commonwealth Drive, Warrendale, Pennsylvania 15086, U.S.A., 201-219.

PARGETER, R. J. (1978), *Weld. Inst. Res. Bull.*, **19**, 325-326.

SVENSSON, L.-E., GRETOFT, B., SUGDEN, A. A. B. and BHADESHIA, H. K. D. H. (1988), 2nd International Conference on "Computer Technology in Welding", Welding Institute, Abington, U.K., in press.

TABOR, D. (1951), *J. Inst. Metals*, **79**, 1-18.

THEWLIS, G., (1987), "3rd International Conference on Welding and Performance of Pipeline Steels", *[Proc. Conf.]*, Welding Institute, Abington, U.K., in press.

TREMLETT, H. F., BAKER, R. G., and WHEATLEY, J. M. (1961), *Brit. Weld. J.*, 8, 437-454.

YANG, J.-R. (1987), Ph.D. thesis, University of Cambridge, U.K.